RESEARCH ARTICLE

{M} acro-molecular
Bioscience
www.mbs-journal.de

Check for updates

High Strength and High Toughness Electrospun Multifibrillar Yarns with Highly Aligned Hierarchy Intended as Anisotropic Extracellular Matrix

Xiaojian Liao,* Valérie Jérôme, Seema Agarwal, Ruth Freitag,* and Andreas Greiner

Electrospun nanofibers can be effectively used as a surrogate for extracellular matrices (ECMs). However, in the context of cellular mechanobiology, their mechanical performances can be enhanced by using nanofibrous materials with a high level of structural organization. Herein, this work develops multifibrillar yarns with superior mechanical performance based on biocompatible polyacrylonitrile (PAN) as surrogate ECM. Nearly perfect aligned nanofibers along with the axis of the multifibrillar yarn are prepared. These highly aligned yarns exhibit high strength, high toughness, good stress relaxation behavior, and are robust enough for technical or medical applications. Further, this work analyzes the influence of the highly aligned-hierarchical topological structure of the material on cell proliferation and cell orientation using cells derived from epithelial and connective tissues. Compared to nonoriented electrospun multifibrillar yarns and flat films, the well-ordered topology in the electrospun PAN multifibrillar yarns triggers an improved proliferation of fibroblasts and epithelial cells. Fibroblasts acquire an elongated morphology analogous to their behavior in the natural ECM. Hence, this heterogeneous multifibrillar material can be used to restore or reproduce the ECM for tissue engineering applications, notably in the skeletal muscle and tendon.

1. Introduction

Fabricating a functional material that closely mimics the natural extracellular matrix (ECM) is a typical tissue-engineering approach because it allows cell organization into a physiologically relevant architecture.[1] Attachment, proliferation, and function of anchorage-dependent cells greatly depend on the physical properties of the underlying substratum.[2] Cells tend to adhere to structures that minimize the distortion of their cytoskeleton.[3] Benefiting from the aligned hierarchical structure in their natural ECMs, skeletal muscle and tendon tissues are strong enough to bear or transfer external forces and store or release energy.[4] For tissue engineering of these tissues, besides the material's biocompatibility, its mechanical flexibility and robustness are critical properties determining its suitability as an artificial ECM.[5] Advanced materials with good mechanical performance are still needed for such ECM surrogates. Whereas high-strength materials have a high resistance to deformation, high toughness (damage-tolerant) materials absorb a lot of energy and deform without breaking.[6] Combining high strength and high toughness in an innovative artificial ECM would be a cutting-edge approach to obtain scaffolds with superior mechanical properties for tissue engineering. However, high strength and high toughness, on the other hand, are usually mutually exclusive in most materials.

Electrospun nanofibers have attracted attention as excellent candidate materials for artificial ECM due to their small diameters, which are in the same order of magnitude as the natural fibers in the ECM (e.g., collagen).[7] Notably, single electrospun polymer nanofibers exhibit a perfect combination of high strength and high toughness.[8] These single nanofibers, however, are not robust enough for technical or medical applications. Consequently, electrospun nanofibers are usually assembled into fibrous structures with various shapes, ranging from fibrous yarns[9] and fibrous membranes[10] to fibrous sponges.[11] Yet, due to the intrinsic chaotic structure of electrospun fibers, the mechanical performance of these assemblies is rather weak. Various approaches, including collecting fibers by a high-speed collector,[12] controlling the fiber deposition by adjusting the electrical field,[13] or mechanically aligning the fibers by stretching,[14] have been used to improve the alignment of fiber. Though the aligned structure in the fibrous membranes or yarns could increase the strength of the corresponding materials, achieving the required combination of high toughness

X. Liao, S. Agarwal, A. Greiner
University of Bayreuth
Macromolecular Chemistry
Bavarian Polymer Institute
95440 Bayreuth, Germany
E-mail: xiaojian.liao@uni-bayreuth.de
V. Jérôme, R. Freitag
University of Bayreuth
Process Biotechnology
95440 Bayreuth, Germany
E-mail: ruth.freitag@uni-bayreuth.de

**ADVANCED
SCIENCE NEWS**

www.advancedsciencenews.com

**Macromolecular
Bioscience**

www.mbs-journal.de

and high strength is still challenging.[14,15] Recently, our group proposed a method for the fabrication of high strength (1236 ± 40 MPa) and high toughness (137 ± 21 J g⁻¹) multifibrillar yarns through a combination of thousands of highly aligned polyacrylonitrile (PAN) fibrils and interfibrillar reactions between the PAN and a small amount of poly(ethylene glycol) bisazide (PEG-BA).[6] These yarns exhibit good fatigue resistance even after 5000 loading and unloading cycles at a maximum tensile strength of 400 MPa, as shown by a negligible change in the final tensile strength (≈5.3%) and plastic deformation (≈4.2%). Due to their excellent mechanical properties, these materials are expected to be well-suited for developing biomaterials for which mechanical stimulation, i.e., the "driving force" of cellular mechanobiology, is essential.

The compatibility of PAN for applications in cell culture has been first recognized in the mid 70's.[16] PAN homopolymer is nontoxic and is highly effective for the attachment and cultivation of various cell types (e.g., human HepG2 hepatoma).[16] Pure PAN homopolymer membranes (i.e., films) provide excellent conditions for human skin fibroblast attachment and spreading.[17] Electrospun PAN, e.g., in form of nonwovens, was reported as a suitable material to support the cultivation and differentiation of stem cells.[18] Recently, PAN has been reported as a promising material for biomedical applications, showing no inflammatory response and de novo cell colonization after subcutaneous implantation in mice.[19]

In this contribution, we investigate the suitability of high strength and high toughness PAN multifibrillar yarns to support cell attachment and proliferation in vitro. Various hierarchical topologies containing different amounts of PEG-BA, used as an interconnecting molecule, were produced. Specifically, we compared nonaligned (i.e., unstretched) and aligned yarns with films prepared with the corresponding polymer. Surface wettability and mechanical properties of the produced materials were analyzed by contact angle measurements and tensile test, respectively. The biocompatibility of the materials was estimated by a standardized (ISO-10993) MTT assay. The spreading and proliferation capability of fibroblasts and epithelial cells on PAN/PEG-BA-based materials were investigated qualitatively and quantitatively by cell staining and AlarmarBlue assay, respectively. Finally, electron microscopy analysis was performed to provide a closer look at the cell-material interaction.
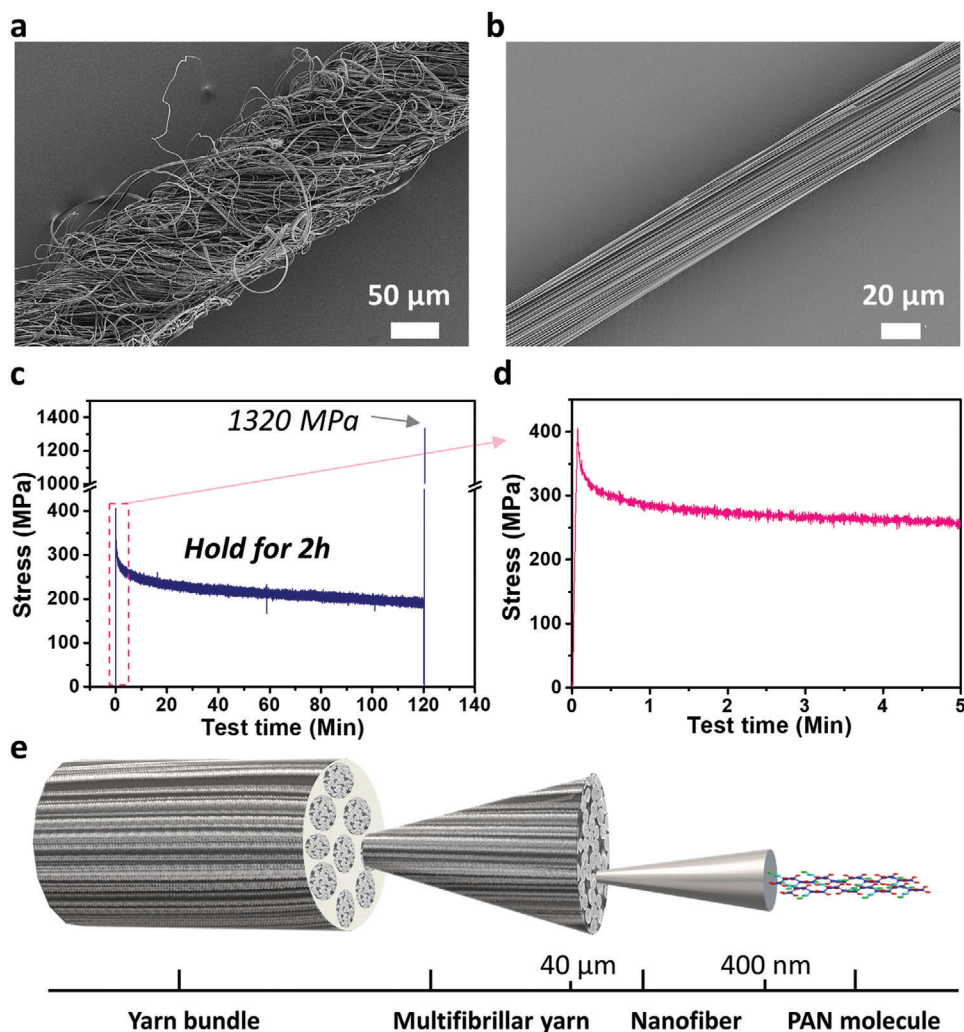
2. Results and Discussion

2.1. Electrospun Multifibrillar Yarns

Continuous as-spun multifibrillar yarns with a diameter of about 130 μm were fabricated by electrospinning. Such yarns consist of approximately 3000 unaligned (with an alignment factor of about 46.0%) individual nanofibers with a diameter of about 1.2 μm, as shown in **Figure** 1a. The subsequent stretching and annealing processes lead to a high-level alignment of the nanofibers, represented by the high alignment factor of about 99.4% at a stretch ratio of 8 (SR8) and a threefold reduction of the nanofiber diameter (400 nm) (Figure 1b). To obtain high strength and high toughness yarns, a small amount of PEG-BA oligomer was added to the yarns. PEG-BA works as a flexible interconnector to covalently bind the nanofibers by cycloaddition reaction between the

azide groups of PEG-BA and the acrylonitrile ones of PAN. The as-spun (unstretched) and annealed (at 130 °C for 4 h) yarns without PEG-BA are designated as EAY and the as-spun yarns processed with PEG-BA, and annealed (at 130 °C for 4 h) are abbreviated as i-EAY. While, the electrospun, stretched (SR8), and annealed yarns without PEG-BA are designated as EASY-X and the yarns processed with PEG-BA, stretched (SR8), and annealed at 130 °C for 4 h are abbreviated as i-EASY-X, where X corresponds to the wt% of PEG-BA. Table S1 (Supporting Information) shows the details abbreviation information of samples. As reported in our previous work,[6] a strength of 72 ± 3.0 MPa was measured for EAY. The combination of stretching (i.e., introduction of high fibril orientation) and annealing with 4 wt% PEG-BA as an interlinking molecule resulted in both high strength (about 1200 MPa) and high toughness (about 137 J g⁻¹). The obtained combination of high strength and high toughness in our materials is similar to the properties of drag-line spider silk. Though our yarns feature a lower strength than the Kevlar fibers, carbon fibers, and CNTs fibers, the toughness is higher, which means our materials can absorb more energy before rupturing. Meanwhile, the toughness of our materials is higher than any other man-made yarns, while their strength is comparable.[6] Though single polymer nanofibers could yield very high strength and toughness,[8] handling a single nanofiber with nanometers diameter has prevented many glorious nanofibers, confirmed in research laboratories, from finding real-world applications in viable and robust forms. Combining thousands of highly aligned nanofibrils perfectly overcomes the problems of single nanofibers. Thus, these robust yarns can be widely used in practical applications.
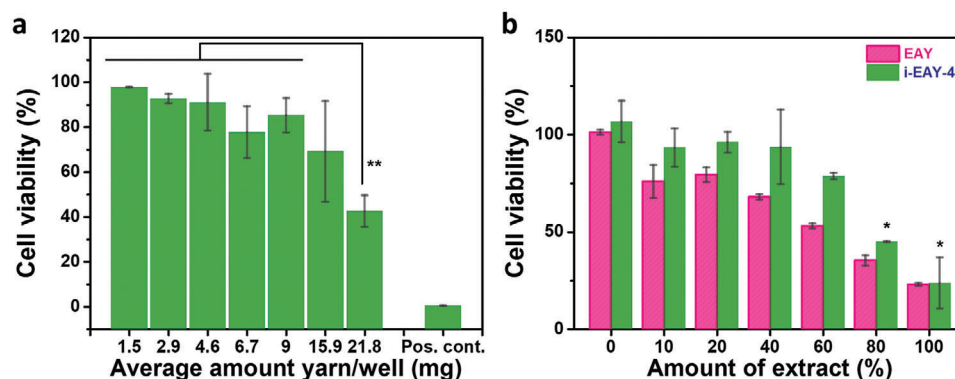
To further investigate the mechanical properties of i-EASY-4 yarns, a stress-relaxation test at a given strain for 2 h was performed, as shown in Figure 1c,d. The i-EASY-4 was tensile-extended until the yield strength, i.e., near 400 MPa was achieved. Then, the stress relaxation kinetic was recorded by keeping this constant strain for 2 h during which the tensile stress steadily decreased to about 190 MPa. A steep stress relaxation from 400 to 300 MPa occurred within the first 0.3 min of the kinetic (Figure 1c,d), followed by a relaxative stress decrease over the remaining analysis time (119.7 min). According to a common assumption in material sciences, a material can return to its prior state when the stress is removed as long as the applied force is below the yield strength. However, when the applied force exceeds the yield strength, the material deformation becomes to a certain extent permanent and irreversible. Such behavior is called plastic deformation. Because of this yarn's yield strength of about 400 MPa,[6] this long-time holding hardly induces defects in the materials. Thus, after this stress–relaxation test, the yarns can still keep high strength (1320 MPa). It also attests to material robustness. Yarns produced here exhibit a hierarchical structure. Highly aligned nanofibers, composed of densely aligned PAN molecules along with the axis of yarns, are assembled into multifibrillar yarns, which are then assembled in parallel into bulk multiyarn bundles (Figure 1e). To some extent, these structures closely mimic the skeletal muscle or tendon hierarchy (Figure S1, Supporting Information). Moreover, the surface roughness of these yarns is in the nanosize range. As recently reviewed, nanoroughness is considered to mirror natural ECM morphology and has a positive effect on cell attachment and proliferation might.[20]

ADVANCED
SCIENCE NEWS
www.advancedsciencenews.com

[M] **acro-**
[M] olecular
Bioscience
www.mbs-journal.de

Figure 1. Microstructure and mechanical properties of electrospun multifibrillar yarns. a,b) Scanning electron microscopy (SEM) images of EAY-4 (a) and i-EASY-4 (b). c) Stress–relaxation test curve of i-EASY-4. When the applied stress of 400 MPa is reached, the i-EASY--4 is held constant strain for 2 h. A tensile test of i-EASY-4 was recorded immediately after the stress–relaxation test. d) Detail of the stress–relaxation test curve during the first 5 min (pink dot line area). e) Schematic representation of the hierarchical structure of yarn bundle, single multifibrillar yarn (diameter of unstretched yarn at 130 μm, and stretched yarn at 40 μm), single nanofiber (diameter of 400 nm) and PAN molecule.

The surface wettability of materials has a massive implication on cell attachment and growth. It has been reported that optimal hydrophilicity is required for supporting efficient cell adhesion and proliferation.[21] The influence of PEG-BA incorporation and material topology (film versus yarn) on the hydrophilicity of the materials was assessed by static water contact angles (WCA) measurements (Figures S2 and S3, Supporting Information). In the film state, PAN is a hydrophilic polymer with a WCA value of (61 ± 2.7)°. The incorporation of 4 wt% PEG-BA in the films led to a slight decrease of the WCA (58 ± 2.7)°, which is not statistically significant ($p = 0.110$) (Figure S2, Supporting Information). Due to the small diameter of the yarns (diameter: ≈40 μm), the assessment of the WCA for a single yarn was technically challenging. Thus, for testing, we aligned the individual yarns into yarn bundles as shown in Figure S3 (Supporting Information). During the test, we observed water permeation into the bundles. The porous inner structure of the yarn bundle, as well as the hydrophilicity

of the PAN polymer, conceivably contribute to this phenomenon. The kinetics of the wetting process was recorded. Independently of the nanofibers' orientation (stretched versus unstretched) or the presence of interconnector molecules, all yarn bundles are visibly wettable within less than 5 s. We found that the wetting time for the EASY material (pure PAN with aligned fibrous structure) was longer (about 4.46 s) than for EAY with a nonoriented structure (about 0.7 s) (Figure S3a,b, Supporting Information). This suggests that the nonoriented structure with bigger pores in the unstretched yarns facilitates water permeation compared to the highly aligned and dense topological structure of the EASY yarns. Moreover, the addition of PEG-BA improved yarn wettability, as shown by a shorter wetting time for both unstretched (i-EAY-4, Figure S3c, Supporting Information) and aligned (i-EASY-4, Figure S3d, Supporting Information) materials compared to the respective without PEG-BA ones (Figure S3a,b, Supporting Information).

2200291 (3 of 12)

**ADVANCED
SCIENCE NEWS**

www.advancedsciencenews.com

⎰M⎱ **acro-
molecular**

Bioscience

www.mbs-journal.de

Figure 2. Cytotoxicity analysis of EAY and i-EAY-4 materials by MTT assay. L929 cells were exposed for 24 h to the culture medium (negative control), material (direct MTT), or extracts prepared from materials (indirect MTT), and Triton-X100 was used as the positive control (Pos. cont.). a) Direct contact method with various amounts of i-EAY-4 yarns. b) Indirect MTT assay with 0 to 100% extracts prepared with EAY and i-EAY-4 yarns. Data represent mean $\pm$ SD (PAN $n = 1$ with two technical replicates; i-EAY-4, $n = 2$ biological replicates). Statistical significance within a group is indicated by [**] $p < 0.001$ and [*] $p < 0.05$. Statistical significance between "15.9 mg" and "21.8 mg" i-EAY-4 treatment is $p = 0.038$.
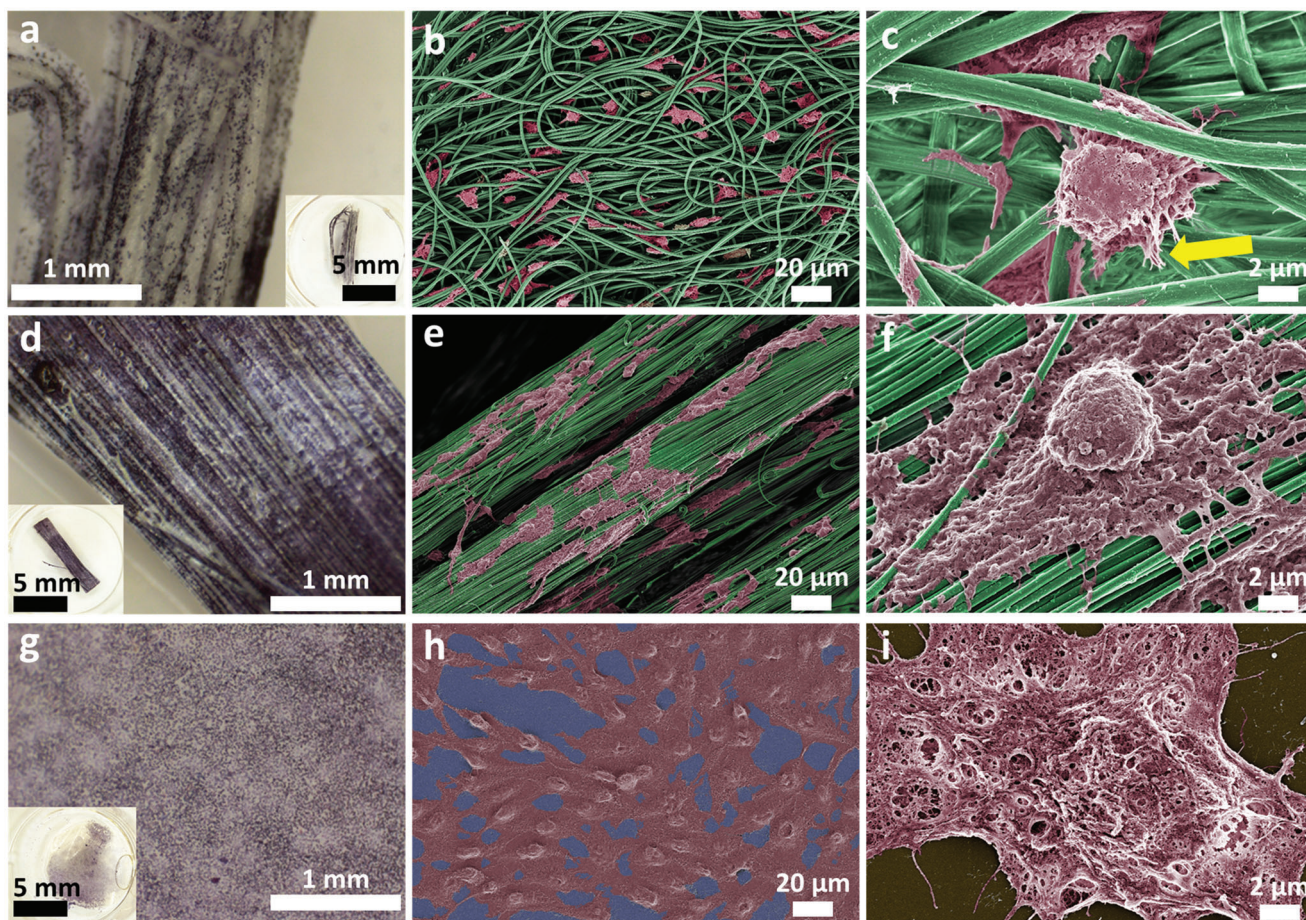
2.2. Cytotoxicity of EAY and i-EAY-4 Yarns on L929

PAN has previously been used in various cell culture applications and generally displayed good cell compatibility.[22] Owing to its hydrophilic and biocompatible properties, PEG has been widely used as an additive for the manufacturing of biodegradable (electrospun) scaffolds.[23] However, to the best of our knowledge, the biocompatibility of PAN/PEG-BA-based materials is not known.

Therefore, we first assessed the cytotoxicity of the EAY and i-EAY-4 yarns by direct MTT assay using the murine fibroblasts cell line L929 as recommended by the ISO guidelines (ISO 10993-5).[24] This cell line has been reported to be more sensitive than primary fibroblasts (e.g., human pulpal fibroblasts) to the toxicity of specific test agents (e.g., zinc oxide-eugenol).[25] L929 cells were seeded into wells of a 6-well plate and cultivated with 1.5 to 22 mg i-EAY-4 bundles per well for 24 h. We restricted our testing to unstretched yarns because the stretching process induces only a physical change of material (i.e., reorientation of the fibers) and hence should not influence its biocompatibility. The viability of nontreated cells (negative control) was set to 100% and compared to the cell survival after exposition to 0.3% Triton X-100 (positive control) and to test samples. The results are presented in **Figure 2**a. As per ISO guidelines, any treatment that reduced cell viability below 70% of the negative controls should be considered to have cytotoxic potential. In cultures exposed to Triton-X100, the viability was always <5%, confirming the responsivity of the cells to a known toxic agent and, hence validating the approach.

Based on the direct MTT assay results, the viability of the L929 cells was $\geq 80\%$ for ≤ 16 mg i-EAY-4 material per well, corresponding to a polymer concentration of 8 mg mL^{-1}. The trend toward reduced cell viability after incubation with 16 mg material per well was not statistically significant. These results reveal good biocompatibility of the material and demonstrate that the introduction of the interconnector PEG-BA into the yarns does not interfere with the previously reported biocompatibility of PAN.[22] Increasing the material amount further (i.e., 22 mg polymer per well, 11 mg mL^{-1}) induces a statistically significant decrease of the cell viability to 40%, indicating some noxious ef-

fects of the i-EAY-4 yarns on the cells. Diffusion hindrance for nutrients/oxygen/metabolites due to large pieces of the material above the cells (i.e., a mass effect) could be responsible for this drop in viability. Moreover, the release of chemicals (i.e., leachables) remaining from the production steps could also negatively influence cell viability.

To clarify this point, we assessed the cytotoxicity of the yarns by indirect MTT assay as recommended by the ISO guidelines (ISO 10993-12).[26] Here, L929 cells were only exposed to "extracts" of the material to estimate the toxicity of putative leaching agents. Extracts were prepared with EAY and i-EAY-4 yarns incubated in a growth medium, choosing the extraction ratio (100 mg mL^{-1}) recommended for irregularly shaped porous materials (low-density materials). Growth medium submitted to a mock extraction (0% extract) was also prepared to assess the influence of the treatment on the growth medium quality. Cells were incubated for 24 h with growth medium containing 0% to 100% extract. To determine the 100% viability, cells were also cultivated in a fresh growth medium under otherwise similar conditions. As shown in Figure 2b, there is only a statistically significant ($p \leq 0.05$) decrease in cell viability for 80% and 100% extracts prepared from the i-EAY-4 material. A trend toward higher toxicity of extracts prepared with the EAY material was detected, indicating that the number of leachables released from the EAY sample was higher than for PEG-BA-containing ones. Altogether these results suggest that a nonnegligible amount of leachables were released in the medium, inducing cytotoxicity. During the nanofibers production, acetone (boiling point: 56 °C) and in particular *N,N´*-dimethylformamide (DMF; boiling point: 153 °C) might not fully evaporate during the electrospinning, stretching, and annealing phase performed at 130 °C. Considering that no toxicity was detected at 10% to 20% extract prepared with 100 mg mL^{-1} material, one can assume that the noxiousness witnessed in the direct MTT for about 11 mg mL^{-1} i-EAY-4 material (Figure 2a) was related to the experimental setting discussed above (i.e., disturbance of the cells' supply) and not to the release of leachables. Overall both cytotoxicity analyses indicate that the prepared materials/yarns are biocompatible and in consequence can be used for cell seeding tests.

**ADVANCED
SCIENCE NEWS**

www.advancedsciencenews.com
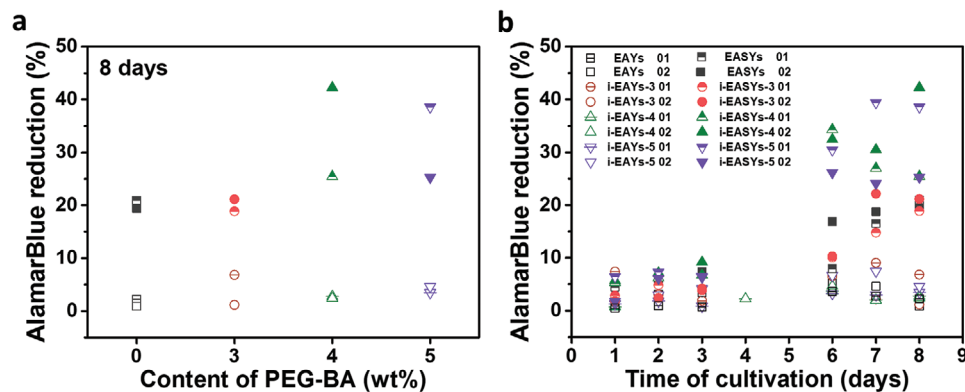
[M]acro-
molecular

Bioscience

www.mbs-journal.de

Figure 3. Microstructures of representative electrospun multifibrillar yarns and films (all processed with 4 wt% PEG-BA) after 8 days of cultivation with L929 cells. Cells inoculation density: 2.6×10^4 cells cm^{-2}. MTT staining of i-EAY-4 yarns (a), i-EASY-4 yarns (d), and film (g). Inserts (a,d,g) are representative of the full samples. Scanning electron microscopy (SEM) analysis at low (b,e,h) and high (c,f,i) magnifications of i-EAY-4 yarns (b,c), i-EASY-4 yarns (e,f), and film (h,i), respectively. Artificial colors were applied to ease visualization (pink: cells; green: fibers). The original SEM pictures are given in Figure S4, Supporting Information). The arrow indicates some wrapping of the cells around the fibers.

2.3. Influence of Material Topology and the PEG-BA Content on Fibroblasts Attachment

Cell attachment and proliferation on a given polymer surface are essential factors that directly influence the suitability of the material for TE applications.[27] As shown above, some remaining leachables from the production process are still present in the yarn bundles and need to be washed away before using these bundles as scaffolds for cell cultivation to avoid experimental bias due to charge variation. Therefore, the yarn bundles were always preincubated in a growth medium containing 10 vol% fetal calf serum at 37 °C for 16–24 h before seeding the cells. Incidentally, besides washing away most of the leachables remaining from the production step, it is expected that this treatment concomitantly allows for serum proteins deposition on materials' surfaces. It is widely accepted that specific proteins in serum promote cell adhesion (e.g., fibronectin). Protein adsorption thus improves the polymer surface's suitability for cell attachment.[28] In the past, we have successfully used such a prewetting step to increase the wettability of poly(MA-co-MMA-co-MABP) and PLA/PCL-based scaffolds.[29] As shown above by WCA measurements, the hy-

drophobicity of the materials was not a concern in the case of the PAN-based yarns. Nevertheless, the preincubation step in the growth medium was expected to further facilitate cell attachment. To investigate cell attachment/proliferation on the electrospun orientated and nonoriented fibers, fibroblasts L929 cells were seeded on i-EASY-4 and i-EAY-4 yarns and cultivated for 8 days, respectively. Thereafter, the samples were stained with MTT to macroscopically assess the cell spreading and further analyzed by scanning electron microscopy (SEM) for a more detailed investigation of the cells/material interaction (**Figure 3**). Films (i.e., regular smooth surface) produced from the same material were also used to evaluate the influence of the material topology (i.e., smooth versus fibrous structure) on cell behavior.

The qualitative analysis of the cell distribution on the yarn bundles (MTT staining) revealed that L929 cells tend to spread homogeneously on the surface of the yarns and films (Figure 3a,d). However, aligned i-EASY-4 yarns and films offer a more favorable environment than the corresponding i-EAY-4 (i.e., nonoriented) one for cell attachment and proliferation (Figure 3a,d,g). Of note, after MTT staining the cells tended to detach from the films but not from the yarns, indicating differences in interaction

2200291 (5 of 12)

**ADVANCED
SCIENCE NEWS**
www.advancedsciencenews.com

{M}acro-
molecular
Bioscience
www.mbs-journal.de

Figure 4. Cultivation of L929 cells on electrospun multifibrillar yarns. Cell proliferation after cultivation on multifibrillar yarns containing 0–5 wt% PEG-BA. Cells inoculation density: 6×10^5 cells per well. Cell proliferation was measured on the given days with AlamarBlue. a) Cell proliferation measured with AlamarBlue on day 8. Presented data issued from independent experimental replicates. b) Kinetic of cell proliferation on multifibrillar yarns with different weight percent of PEG-BA. EAY-X/i-EAY-X yarns (unstretched, empty symbols); EASY-X/i-EASY-X yarns (stretched, solid symbols). Presented data issued from two independent experimental replicates ($n = 2$). Identical symbols were used in both panels.

strength between cells and materials. A subsequent SEM analysis of the samples reveals major differences in the morphology of the cells grown on various materials. Whereas the cells tend to be round-shaped in the context of i-EAY-4 (Figure 3b,c), they display a flattened morphology (Figure 3h,i) with an elongated triangular morphology characteristic for fibroblasts (Figure 3h) when grown on films. After cultivation on aligned fibers (i-EASY-4) (Figure 3e,f), cells display also a flattened morphology. Of note, in the case of unstretched yarns, the cells tended to enclose the fibers (Figure 3b,c).
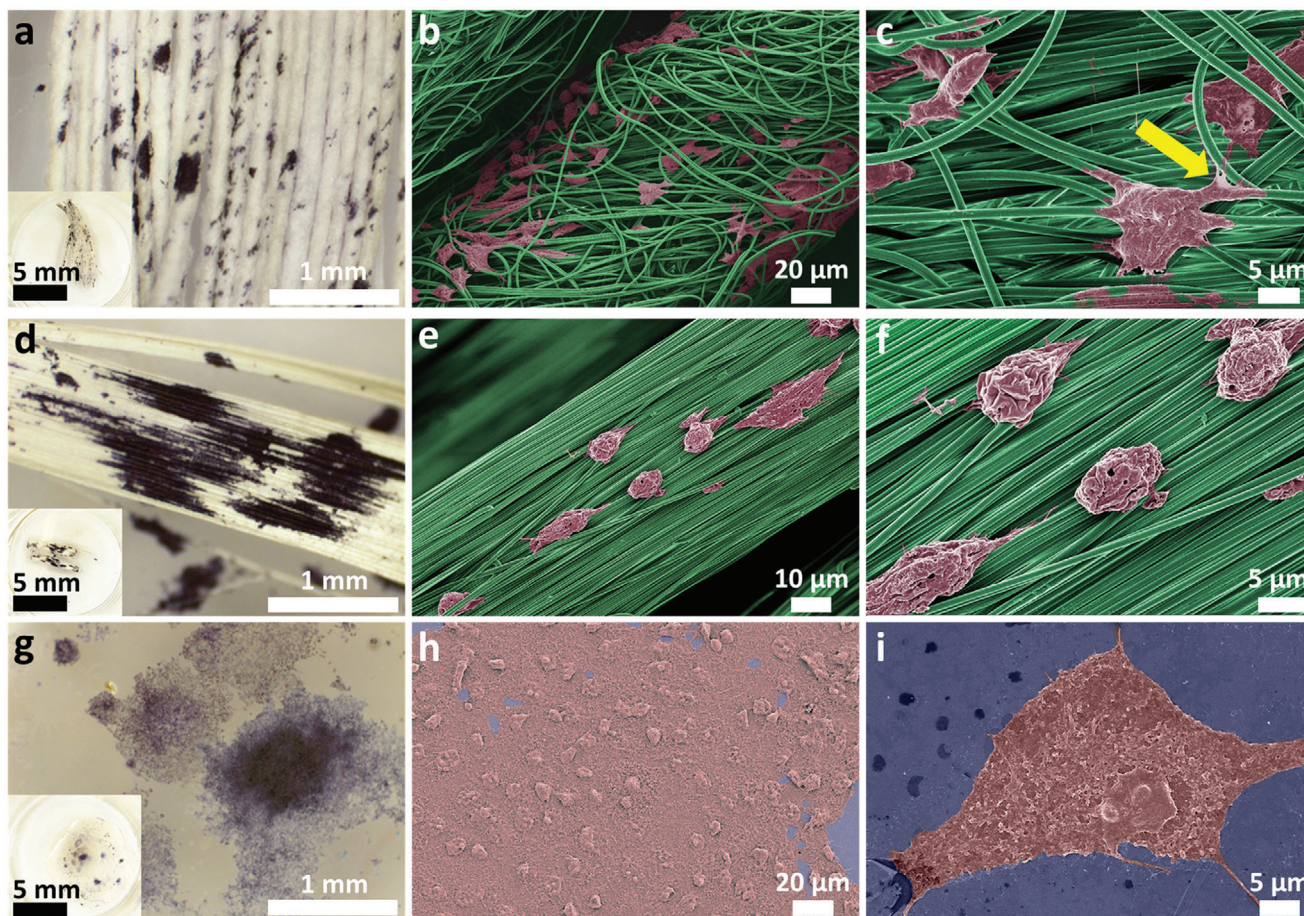
In a subsequent experiment, we investigated the influence of the amount of PEG-BA (0, 3, and 5 wt%) on the cell morphology by SEM analysis (Figures S5 and S6, Supporting Information). The results confirmed the observations made with i-EAY-4 and i-EASY-4. Independently of the amount of PEG-BA in the yarns, the cell attachment was improved on stretched materials. Hence, the amount of interconnector molecules during the yarn processing has little influence on the cell adhesion property of the material. Interestingly, the SEM images suggest that the cells aligned along the aligned fibers. Such behavior is known as contact guidance[30] Altogether, these results allow hypothesizing that for the unstretched material, the spacing of the fibers is in most cases not suitable to accommodate a proper binding of the cells (i.e., the distance between anchoring points is not adequate). For the stretched material, the distance between the fibers is narrow and hence exhibits a rough surface which has been described in the past to be most suitable for cell attachment.[20]

2.4. Influence of PEG-BA Content on L929 Cells Proliferation

Next, we investigated to which extent the amount of PEG-BA could influence cell proliferation. Using an experimental setting analogous to the one used in Figure 3, we quantified the cell proliferation after 8 days of cultivation on nonstretched and stretched yarns prepared with 0% to 5% PEG-BA. The cell proliferation was quantified using the AlamarBlue assay.[31] The data presented in **Figure 4**a proved the suitability of the stretched yarns to support L929 cell proliferation and incidentally confirm that the stretch-

ing process does not change the biocompatibility of the materials. The variation among the biological replicates could, to some extent, be associated with a nonhomogeneous binding of the cells to the materials during the seeding phase. Further, there is a trend toward an improved proliferation on yarns processed with PEG-BA amounts >3 wt%. These results are in line with previous studies showing that modulation of cell adhesion on electrospun fibers, such as polyamide and PCL, can be achieved by blending in various amounts of PEG.[21b,25a]

Taking the advantage that AlarmarBlue is a nondestructive, nontoxic, and repetitive method,[31] we subsequently analyzed the growth kinetic of L929 cells on specific multifibrils bundles containing 0% to 5 wt% PEG-BA over 8 days of cultivation (Figure 4b). The results confirmed that L929 cells proliferate better on the stretched yarns. If at all, unstretched yarns only support low cell proliferation over the analyzed cultivation time. Major proliferation differences between the i-EASY and EAY materials become discernable after 6 days of cultivation. Hence, the development of cell proliferation on i-EASY displays a biphasic growth behavior, indicating that the cells need to first adapt to the material surface. In comparison, cells seeded at the same density and cultivated in parallel under standard conditions in tissue culture plates displayed a monophasic growth (Figure S7, Supporting Information). The biphasic proliferation behavior is observed independently of the amount of PEG-BA incorporated in the yarns. As observed in the former experiment (Figure 4a), cell proliferation on yarns containing 4–5 wt% PEG-BA is generally higher than for EAYs yarns or yarns containing less PEG-BA. As previously published, pure PAN nanofibers do not promote cell adhesion, while PAN blending with additives (e.g., gelatin) improves cell attachment.[32] Moreover, it is usually accepted that incorporating PEG improves the biocompatibility of materials for tissue engineering.[33] Our data demonstrate that oriented fibers provide a good surface supporting fibroblasts' proliferation (i.e., L929 cells), particularly after modification with PEG-BA. In vivo, fibroblasts are present in connective tissues,[34] where they bind to the proteinous fibers (e.g., collagen) of the ECM. Here, the highly aligned i-EASY-X materials supposedly mimic this in vivo environment.

**ADVANCED
SCIENCE NEWS**

www.advancedsciencenews.com

[M] acro-
molecular
Bioscience

www.mbs-journal.de

Figure 5. Microstructures of representative electrospun multifibrillar yarns and films (4 wt% PEG-BA) after 8 days of cultivation with HuH7 cells. Cells inoculation density: 2.6×10^4 cells cm^{-2}. MTT staining of i-EAY-4 yarns (a), i-EASY-4 yarns (d), and film (g). Inserts (a,d,g) are representative of the full samples. Scanning electron microscopy (SEM) analysis at low (b,e,h) and high (c,f,i) magnifications of i-EAY-4 yarns (b,c), i-EASY-4 yarns (e,f), and film (h,i). Artificial colors were applied to ease visualization (pink: cells; green: fibers). The original SEM pictures are given in Figure S8 (Supporting Information). The arrow indicates some wrapping of the cells around the fibers.

2.5. Influence of Material Topology on Epithelial Cells Attachment

To assess if the improved proliferation of the L929 cells on the aligned yarns was related to their fibroblast phenotype, we extended our study to epithelial cells. These cells form epithelial tissues, which display in vivo ordered structures with tightly packed polarized cells (i.e., cell–junction, apical, and basal poles) embedded in very little ECM and bound to a basement membrane via the basal pole of the cells.[35] HuH7 cells (hepatoma cells, i.e., liver epithelial cancer cells) were cultivated on i-EAY-4 yarns, and i-EASY-4 (**Figure 5**). Film (i.e., regular surface) produced from the same materials was again used to evaluate the influence of the material topology on cell behavior. To allow for comparison with the results obtained for L929 cells (Figure 3), the HuH7 seeding cell density was also set at 2.6×10^4 cells cm^{-2}. After 8 days of cultivation, the distribution of HuH7 cells was first estimated qualitatively by staining the samples with MTT dye (Figure 5a,d,g).

HuH7 cells did grow on all investigated materials, although it should be mentioned that after MTT staining the cells again tended to detach from the films but not from the yarns. This in-

dicates that, as for the fibroblasts, the strength of cell adhesion to the materials was higher for the yarns than for the films. This might be ascribed to the roughness of the yarn's surface. The topographic reaction (i.e., reaction to the surface landscape) of cells to micrometer-range features has been well established for decades.[36] As observed before for the fibroblasts, the spreading of epithelial cells on i-EASY-4 was better than on i-EAY-4. Hence, the aligned surface topology also favors the adhesion of epithelial cells. Remarkably, epithelial cells tended to grow in clusters. SEM analysis of unstretched i-EAY-4 yarns and films revealed no major differences between the two cell lines/types. HuH7 cells also tend to encase the fibers when grown on unstretched material (Figure 5b,c). On films, the cells were flattened, indicating a large adhesion surface to the material (Figure 5h,i). On both types of yarn, HuH7 cells tended to be round-shaped (Figure 5e,f) and did not align along with the fibers when grown on stretched yarns. In this context, the contact area between the cells and stretched material was twofold lower for the HuH7 cells than for the L929 ones. Such differences in behavior might be related to the respective structure of the natural ECM for both cell types.

In vivo, fibroblasts are located in connective tissues and hence in contact with a meshwork of collagen fibers.[37] Epithelial cells are connected to anchoring filaments (i.e., thread-like structures made of a high amount of laminins and dystroglycan) traversing the upper part of the basement membrane, the so-called lamina lucida.[38] Hence, whereas fibroblasts are used to adhere to oriented fibers in some tissues (e.g., tendon), epithelial cells do not. Yet, our results suggest that the intrinsic topology of the material and not its chemistry is accountable for reproducing a natural ECM environment, which is recognized by the cells according to their phenotype.

2.6. Proliferation of Fibroblasts versus Epithelial Cells on i-EAY-4 and i-EASY-4 Multifibrillar Yarns and Films

Finally, we performed a side-by-side quantitative estimation of L929 and HuH7 cell proliferation on identical batches of PAN/4 wt% PEG-BA materials. For comparison, we analyzed the proliferation of both cell lines in standard tissue culture plates (i.e., surface-treated polystyrene, $PS_{treated}$). This was an important control to disclose putative differences that might only be due to variation in the proliferation rate of the cells. As published elsewhere, L929 cells have a cell population doubling time (t_d) of 28 h.[39] HuH7 cells have a t_d of 36 h as measured by our group.[29b] The quantitative analysis of cell proliferation is presented in **Figure 6**.

After 3 days of cultivation under standard conditions in a 24-well tissue culture surface-treated polystyrene plate, an average of 5.9×10^5 and 1.5×10^5 cells were recorded for L929 and HuH7 cells, respectively. This result shows that the overall proliferation of the fibroblasts is about fourfold higher than for the epithelial cells. This can be ascribed to the lower t_d of the L929 cells, i.e., a faster proliferation rate. For both cell lines, the proliferation on films ($Mean_{L929}$: 1.8×10^5 cells, $Mean_{HuH7}$: 0.2×10^5 cells) was $\geq$ 2.4-fold lower than on the $PS_{treated}$ surface. As mentioned above, the cell adhesion on films was generally weak, yet higher for the fibroblasts compared to the epithelial cells. This may have led to some experimental bias due to an uncontrollable cell loss during cell handling (e.g., medium change). Still, these results show that the PAN/4 wt% PEG-BA film is less suitable than the $PS_{treated}$ surface (i.e., tissue culture plates) for L929 and HuH7 cultivation. However, the proliferation difference on films between the two cell lines was higher (i.e., ninefold) than in the case of the $PS_{treated}$ culture plates, suggesting that the PAN/4 wt% PEG-BA material is more suitable for fibroblasts than for epithelial cells. We can hypothesize that fibroblasts can bind better to the PAN/4 wt% PEG-BA material resulting in a reduced cell loss during handling.

For a given cell line, the proliferation on yarns is tendentially better than on films but not as good as on the $PS_{treated}$ culture plates in most cases. The proliferation of L929 cells on i-EASY-4 is improved compared to unstretched material (i-EAY-4) but was still below the values obtained with the $PS_{treated}$ surface. Whereas proliferation of HuH7 cells on i-EASY-4 and 24-well plate was similar (no statistical difference, $p = 0.115$), their proliferation on films was similar to the unstretched yarns (no statistical difference, $p = 0.425$). On i-EAY-4 (non-oriented fibers), L929 cells grow better than HuH7 ones ($Mean_{L929}$: 2.5×10^5 cells,
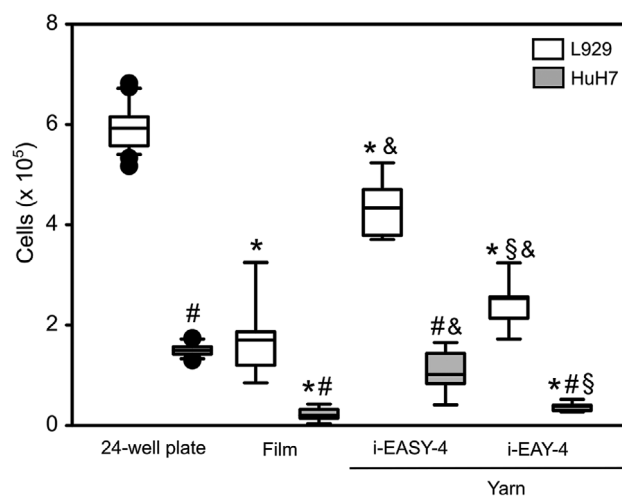
Figure 6. Cultivation of L929 and HuH7 cells on 24-well plate, films, and yarns. 24-well plate: surface-treated polystyrene. Film and yarns: PAN/4 wt% PEG-BA. Cells inoculation density: 2.6×10^4 cells cm^{-2}. Cell proliferation was measured by MTT assay after 72 h of cultivation. Therefore, the formazan crystals produced during the MTT assay were dissolved, and the absorption at 580 nm was measured. L929 cells (fibroblast, white); HuH7 cells (epithelial cells, gray). Presented data issued from six independent experimental replicates ($n = 6$). Statistical significance between PS-treated surface (24-well plate) and PAN/4 wt% PEG-BA-based materials (Films, yarns) is indicated as $^*p < 0.001$. Statistical significance between "L929" and "HuH7" groups for a given cultivation type is indicated as $^\#p < 0.001$. Statistical significance between "i-EASY-4" and "i-EAY-4" groups for a given cell line is indicated as § (L929: $p < 0.001$; HuH7: $p = 0.007$). Statistical significance between "Film" and "Yarn" groups for a given cell line is indicated as & (L929: $p = 0.007$; HuH7: $p < 0.001$). The number of cells was extrapolated from calibration curves (Figure S9, Supporting Information).

$Mean_{HuH7}$: 0.4×10^5 cells), and the difference in proliferation between L929 and HuH7 (6.5-fold) is higher than determined for $PS_{treated}$ culture plates. Using aligned fibers (i-EASY-4) improved the cell proliferation in both cases ($Mean_{L929}$: 4.3×10^5 cells, $Mean_{HuH7}$: 1.1×10^5 cells), and a 3.9-fold increase in cell number was observed for L929 compared to HuH7 cells. Altogether, the difference in proliferation between L929 and HuH7 cells is higher for films (ninefold) and unstretched yarns (6.5-fold) than for the standard tissue culture material (fourfold), indicating that PAN/PEG-BA (4 wt%) better support fibroblast proliferation. Moreover, the proliferation of fibroblasts on i-EASY-4 is only 1.4-fold lower than in the tissue culture plate, suggesting that this material is highly suitable for fibroblast cultivation.

3. Conclusion

We showed that the interconnector PEG-BA used to increase the strength and toughness of PAN-based electrospun yarns slightly increases the material's wettability and improves biocompatibility, as shown by standard MTT assay. In terms of material structure, compared to unstretched i-EAY-X multifibrillar yarns, aligned (i-EASY-X) multifibrillar yarns improve fibroblasts' attachment, proliferation, and orientation. Of note, PEG-BA positively influences fibroblast proliferation in a concentration-dependent manner only in the case of aligned multifibrillar

**ADVANCED
SCIENCE NEWS**

www.advancedsciencenews.com

[M]acro-
molecular
Bioscience

www.mbs-journal.de

yarns. Moreover, we demonstrated that electrospun nanofibers assembled into highly aligned-hierarchical multifibrillar structures (i-EASY-X) are not only well-suited to support the cellular proliferation of fibroblasts (i.e., cells resident in the connective tissues) but also allow cultivation of hepatoma cells (i.e., epithelial cells). Comparing the proliferation behavior of fibroblasts and epithelial cells on i-EASY-X allows us to hypothesize that the intrinsic topology of the material and not its chemistry is accountable for the mimicking of a natural ECM environment, which is recognized by the cells according to their phenotype. To conclude, we developed a cutting-edge material with unique combined properties of biocompatibility, high alignment, hierarchy, as well as high mechanical strength, toughness, and stability that could in the future be of high interest for the replacement of fibrous connective tissues (e.g., tendon tissue engineering).

4. Experimental Section

Materials: PAN (M_n of 120 000, co-polymer with 6 wt% methyl acrylate, Dolan, Germany), poly(ethylene glycol) bisazide (PEG-BA; M_n of 1100; Sigma–Aldrich, Taufkirchen, Germany), DMF (99.99%; Fisher Chemical, Germany), and acetone (Sigma-Aldrich, ≥99.5%) were used as received. If not otherwise indicated, Greiner Bio-One (Frickenhausen, Germany) was used as a supplier for cell culture materials. Trypan blue solution (0.4%) was from VWR (Ismaning, Germany). Minimum Essential Medium Eagle (MEM) with and without phenol red, Dulbecco's phosphate-buffered saline without Ca^{2+} and Mg^{2+} (DPBS), fetal calf serum (FCS), L-glutamine, penicillin, and streptomycin were from Biochrom AG (Berlin, Germany). AlamarBlue solution was from Bio-Rad (Feldkirchen, Germany). 3-(4,5-dimethyl-2-thiazolyl)-2,5-diphenyl-2H-tetrazolium bromide (MTT), paraformaldehyde, and glutaraldehyde solution (grade I, 70%), Triton-X100, Na cacodylate, and $MgCl_2$ were from Sigma–Aldrich.

Methods: *Fabrication of Multifibrillar Yarn Bundles*: The electrospun multifibrillar yarns were fabricated following the previously published method.[6] The electrospinning solution (15 wt%) was prepared by dissolving 2.0 g PAN powder and 0.08 g poly(ethylene glycol) bisazide (the weight according to the content of PEG-BA to PAN, here is up to 4 wt%) in 9.4 g DMF with 1.93 g acetone. The yarns were fabricated with a homemade setup including two syringe pumps, a high-voltage DC (direct current) power source, a poly(vinyl chloride) (PVC) funnel (8.0 cm in diameter) with a motor controller, and a yarn winder collector (1.73 cm in diameter). Two syringes with the solution were connected separately to the positive and negative electrodes of the DC power supply. The feed rate was 0.5 mL h^{-1}, and the applied voltage was 12 kV (positive pole: +12 kV; negative pole: −12 kV). After turning on the electric field, two oppositely charged fibers flew to the funnel at 1500 rpm rotation speed. A continuous yarn was drawn by a presuspended yarn, which was connected with the winder collector with the rotation speed set at 13 rpm. The whole electrospun yarn process was operated under an infrared lamp (250 W) at about 45 °C and with 10%–15% humidity. After electrospinning, in some cases, electrospun yarns (nonoriented) were stretched at 160 °C by a homemade heat-stretching instrument consisting of three parts: a tubular furnace with one heat position zone (Heraeus, D6450 Hanau, Typ: RE 1.1, 400 mm in length, Germany), two rollers controlled by electronic motors, and a laptop with "LV2016" software used to precisely control the velocities of the motors.

Equation (1) was used to calculate the stretch ratio:

$$SR = V_f/V_s \tag{1}$$

where V_f and V_s represent the velocities of fast roller and slow roller, respectively.

The subsequent annealing process was performed by wrapping the curable yarns (unstretched or stretched) around a glass tube (2 cm diameter). The cycloaddition reaction between PAN and PEG-BA was achieved by the azide-nitrile "click" reaction at 130 °C for 4 h. Thereafter, the final yarns were quickly transferred to a freezer at −4 °C for 20 min. These yarns are referred to as "i-EAY-X" (unstretched ones) and "i-EASY-X" (stretched ones), where X corresponds to the wt% of PEG. Some yarns were annealed without the addition of PEG-BA and are referred to as "EAY" (unstretched ones) and "EASY" (stretched ones) (Table S1, Supporting Information).

PAN film with 4 wt% PEG-BA was produced as follows: A solution was prepared by dissolving 1.00 g PAN powder and 0.04 g PEG-BA in 6 g DMF. Then, the solution was cast on the glass plate and dried in the fume hood for 12 h at room temperature. Dry solid films were obtained after vacuum drying at 80 °C for 24 h. After being annealed at 130 °C for 4 h, the final films were removed from the glass plate.

Yarns (aligned on the glass tube) and films were washed three times with ethanol and water, respectively. Then, the yarns and films were dried in the vacuum oven at 60 °C for 24 h. The dry yarns were cut into short aligned bundles (length about 1.5 cm) from the glass tube using a scalpel, and the films were cut into short strips (length about 1.5 cm; width about 0.5 cm). Then, these aligned yarn bundles and films were further treated with UV light (254 nm) for 4 h to decrease the bioburden and stored under sterile conditions until use.

Cells and Maintenance: L929 cells (murine fibroblasts, CCL-1, ATCC) were maintained in MEM culture medium (with phenol red), supplemented with 10% fetal calf serum, 4×10^{-3} M L-glutamine, 100 units mL^{-1} penicillin, and 100 µg mL^{-1} streptomycin (M10). HuH-7 human liver cells (hepatocellular carcinoma cell lines generous gift from Dr. Di Fazio, Marburg, Germany) were maintained in DMEM culture medium, supplemented with 10% fetal calf serum, 2×10^{-3} M -glutamine, 100 units mL^{-1} penicillin, and 100 µg mL^{-1} streptomycin (D10). Cells were cultivated at 37 °C in a humidified 5% CO_2 atmosphere. Cells were collected by trypsinization according to standard cell culture laboratory procedure. If not otherwise stated, the culture medium was exchanged every second day during cultivation. Cell numbers and viabilities during passaging and seeding steps were evaluated using a hemocytometer by trypan blue exclusion assay (Neubauer Improved, VWR International).

Cell Seeding and Cultivation on Electrospun Multifibrillar Yarns and Films: Pieces of sterilized (UV-254 nm, 4 h) multifibrils-bundles and films were placed into the wells of cell repellent tissue culture 24-well plates (Greiner Bio-One). The samples were pre-incubated in the cell's respective growth medium at 37 °C for 16 to 24 h to remove putative leachables and to increase the hydrophilicity of the PAN material by nonspecific adsorption of the serum proteins onto the surface of the material. After discarding the growth medium, 2.6×10^4 cells cm^{-2} (estimated sample accessible surface) were carefully dispersed over the surface of the samples. This cell number was chosen according to the recommended seeding cell density for standard tissue culture plates. Control cultures, performed in standard tissue culture plates, were run in parallel under otherwise identical conditions. The seeded samples and the controls were then transferred to the cell culture incubator (37 °C, 5% CO_2, 95 % humidity) for 60 min to allow cell adhesion. An amount of 100 µL of growth medium was then added to each well. After a further 5 h of incubation, an additional 900 µL of growth medium was carefully added along the side of the well to cover the sample. Well-plates were placed back in the incubator, and the cells were cultured for the indicated amount of time.

The proliferation of the L929 cells on the multifibrillar yarns was analyzed daily by AlarmarBlue (AB) assay. After the AB assay, the bundles were rinsed twice with growth medium and further cultivated in fresh growth medium. For this purpose, the plate was placed back into the cell culture incubator.

In some cases, the cell-seeded samples were stained with MTT solution to visualize cell spreading and estimate overall cell proliferation (see below "visualization of cell spreading"). As a reference, the cells were also seeded analogously in standard tissue culture 24-well plates. For calibration of the assay, the cells collected in the exponential growth phase by trypsinization and recovered by centrifugation (200 g, 5 min) were seeded at 0.05 to 1.0 × 10^6 cells per well (1 mL culture medium; four wells were prepared for each

2200291 (9 of 12)

**ADVANCED
SCIENCE NEWS**

www.advancedsciencenews.com

**Macro-
molecular
Bioscience**

www.mbs-journal.de

cell density) in 24-well plates, and subsequently cultivated for 24 h in the cell culture incubator. After that, cells were either collected by trypsinization and counted by trypan blue exclusion assay or stained with MTT (1 mg mL^{-1}) as described below (see "cytotoxicity assay"). In both cases, four independent replicates performed in quadruplicate were analyzed for each cell line. Calibration graphs were prepared by plotting the A$_{580nm}$ versus the number of cells. The regression equations derived from linear fitting of all data points were $y = 5.18 \times 10^{-6} x - 0.05$ (r^2: 0.970) and $y = 1.9 \times 10^{-6} x + 0.02$ (r^2: 0.913) for HuH7 cells and L929, respectively (Figure S9, Supporting Information). In the subsequent analyses, only data points that fell within the standard curve range were retained.

Mechanical Properties Tests: Tensile tests were performed by a tensile tester (zwickiLine Z0.5, BT1-FR0.5TN.D14, Zwick/Roell, Germany) with a clamping length of 10 mm, a cross-head rate of 5 mm min^{-1} at 25 °C, and a pre-tension of 0.005 N. The load cell was a Zwick/Roell KAF TC with a nominal load of 20 N. The two ends of the yarn samples were fixed by double side tapes and placed between the two clamp stages with the top clamp stage applying uniaxial tension on the yarn samples along the vertical direction. The yarn tensile tests were performed by a test program of yarn shape for cross-section calculation, while the linear density and density of the specimen material were input parameters. The stress relaxation tests were performed at maximum stress of 400 MPa with a constant strain for 2 h. The sequential stress of yarn, test time, stain, and work were recorded. After the stress relaxation test, the final stress–strain tensile tests were performed automatically until the yarns ruptured.

Contact Angle Measurement: The contact angles were measured at 25 °C using a drop shape analyzer DSA25S from Krüss. Before the measurements, the yarns were aligned into a bundle and fixed on a glass plate by tape. The films were cut into squares (2 × 2 cm) and tightly taped (both sides) on the glass plate. Milli-Q water drop size was controlled to 5 µL. The circle fit was used with Drop Shape Analyzer (Krüss Advance, v1.3.1) software for the calculations.

AlamarBlue Proliferation Assay: The estimation of cell proliferation with AlarmarBlue (AB) was performed according to the manufacturer's instructions. Briefly, the bundles were transferred to fresh 24-well plates before performing the assay to ensure that only the metabolic activity of cells attached to the yarns was measured. AB working solution (10 vol%) was prepared in fresh cell culture medium. The AB containing medium was added to each well. Incubation was performed for 2 h at 37 °C in the cell culture incubator. Wells without cells served as a negative control. To determine the fluorescence to be expected from the fully reduced form of the AB (positive control), AB solution (10 vol%) made up in the nonsupplemented cell culture medium was autoclaved for 15 minutes (121 °C, 15 psi), as recommended by the manufacturer. Aliquots of the cell culture medium and positive and negative controls were collected, and their fluorescence (Ex. 535 nm/Em. 590 nm) was analyzed in triplicate in a plate reader (Genios Pro, Tecan Deutschland GmbH, Crailsheim, Germany).

Cytotoxicity Assay: Cytotoxicity tests were conducted by MTT (3-(4,5-dimethylthiazol-2-yl)-2,5-diphenyltetrazolium bromide) tetrazolium reduction assay (MTT assay) according to ISO 10993-5[24] and ISO 10993-12[26] guidelines (direct contact and indirect contact).

For the direct MTT assay, L929 cells were seeded at 2×10^5 cells per well (2×10^5 cells mL^{-1}) in six well-plates, and the bundles (initially sterilized by 4 h UV treatment) were added 24 h afterward. After another 24 h of incubation, the culture medium and bundles were removed from the culture plates and each well was rinsed with DPBS and incubated at 37 °C for 2 h with 1.0 mg mL^{-1} MTT in MEM without phenol red to assess cellular vitality. The mitochondria of metabolically active cells convert MTT into purple formazan crystals. The formazan crystals were dissolved in 1 mL isopropanol for 5 min at room temperature under agitation followed by measuring the absorption at a wavelength of 580 nm (A$_{580}$; reference wavelength 670 nm). Cells incubated without bundles or with 1% Triton-X100 were used as negative and positive controls, respectively.

The indirect MTT assay was intended for the analysis of the cytotoxicity of chemicals putatively leaching out of the bundles. The surface area of bundles cannot be precisely quantified due to their configuration; hence a mass/volume ratio of extracting fluid was used. For this purpose, bundles were initially sterilized (4 h of UV light treatment). Each test sam-

ple was soaked in M10 medium at 37 °C for 24 h inside conical tubes placed on a rotator − Extraction ratio: 100 mg mL^{-1}. Thereafter, the extracts were further diluted to 10%, 20%, 40%, 60%, and 80% using fresh M10 medium or used without dilution (100 %). As a negative control (0 %), M10 medium was incubated in a comparable vessel and subjected to identical incubation conditions without material. Subsequently, L929 cells were seeded into 96-well plates at a density of 10^4 cells per well and incubated overnight for attachment. The culture medium was then replaced by the sample extracts (100 µL well^{-1}), and cells were incubated further for 24 h. After that, the medium/extract mix was discarded, and 50 µL MTT solution (1.0 mg mL^{-1}) was added to each well. The culture was then incubated for another 2 h at 37 °C. Then, the MTT solution was removed, and 100 µL isopropanol was added to each well. The plate was incubated for 5 min at room temperature under agitation, and then absorbance was read at 580 nm (reference wavelength 670 nm).

Equation (2) was used to calculate the reduction in culture viability of cells exposed to samples in comparison to cell culture viability of control:

$$\%\text{Viability} = \left(100 \times \text{Abs}_{580\,\text{sample}}\right) / \text{Abs}_{580\,\text{untreated}} \qquad (2)$$

where Abs$_{580\,\text{sample}}$ is the average absorption of the respective groups that were in contact with bundles or given amounts of extract; Abs$_{580\,\text{untreated}}$ is the average absorption of all wells of "negative control".

Electrospun multifibrillar bundles were considered to have cytotoxic potential when the cell culture viability decreases to <70% compared to the control, which was set at 100% viability. Finally, the average viability percentages were obtained for each group based on the outcomes of the three repetitions of each experiment. Group data are reported as mean ± SD.

Visualization of Cell Spreading: At the indicated time, the cultivated bundles or films were carefully rinsed with DPBS, placed in fresh well plates, and incubated at 37 °C (cell culture incubator) for 2 h with 1.0 mg mL^{-1} MTT in MEM without phenol red. MTT is converted by the mitochondria of metabolically active cells into purple formazan crystals and therefore allows a qualitative assessment of the cellular location on bundles and films. For analysis, the MTT-stained samples were observed with a stereo-microscope (SMZ745T, Nikon, Amsterdam, Netherlands) and SEM (Zeiss LEO 1530, Gemini, Germany). For stereo-microscopy, the images were acquired with the software NIS-Elements D version 5.02.03 (Laboratory Imaging s.r.o., Praha, Czech Republic).

Scanning Electron Microscopy: The morphology of the materials was visualized by SEM with a Zeiss LEO 1530 (Gemini) microscope equipped with a field emission cathode and a secondary electron (SE2) detector. Before SEM measurement, all yarn samples were sputter-coated with platinum (thickness: 2.0 nm) by a Cressington 208HR high-resolution sputter coater equipped with a quartz crystal microbalance thickness controller (MTM-20). SEM images were recorded with an acceleration voltage of 3 kV and a working distance of 5.0 mm. The SEM images were used to study the diameter and morphology of the fibrils and yarns.

Cells grown on yarns and films were also analyzed by SEM. Therefore, samples were extensively rinsed with DPBS and incubated for 60 min at room temperature in fixation buffer (2.5 vol% glutaraldehyde − 2.0 vol% paraformaldehyde − 0.1 M Na cacodylate pH 7.2 − 3 × 10^{-3} M MgCl$_2$) under agitation. Fixed samples were then submitted to three washing steps (0.1 Na cacodylate pH 7.2 − 3 (w/v)% sucrose − 3 × 10^{-3} M MgCl$_2$) before dehydration by slow water replacement using a series of ethanol/water solutions (35, 50, 75, and 95 vol%) for 15 min each and final dehydration in absolute ethanol for 15 min. The imaging of the SEM samples was performed with Smart SEM User Interface software (Zeiss, Gemini).

Statistical Analysis: Group data are reported as mean ± standard deviation. If not otherwise stated, n represents the number of independent experiments. OriginPro software (version 2021, OriginLab, Northampton, MA, USA) was used for One-way ANOVA with Holm–Sidak multiple comparison tests to determine whether data groups differed significantly from each other. Statistical significance was defined as $^*p < 0.05$, $^{**}p < 0.01$, and $^{***}p < 0.001$.

**ADVANCED
SCIENCE NEWS**

www.advancedsciencenews.com

**Macro-
molecular
Bioscience**

www.mbs-journal.de

Supporting Information

Acknowledgements

Conflict of Interest

The authors declare no conflict of interest.

Author Contributions

X.L. and V.J. contributed equally to this work. X.L., V.J., R.F., A.G. conceived and designed the experiments. X.L. and V.J. performed the experiments. X.L. and V.J. analyzed the data. X.L., V.J., R.F., and A.G. wrote the paper.

Data Availability Statement

The data that support the findings of this study are available in the supplementary material of this article.

Keywords

anisotropic, electrospinning, extracellular matrix, high strength, high toughness

[1] a) G. S. Hussey, J. L. Dziki, S. F. Badylak, *Nat. Rev. Mater.* **2018**, *3*, 159; b) A. Satyam, M. G. Tsokos, J. S. Tresback, D. I. Zeugolis, G. C. Tsokos, *Adv. Funct. Mater.* **2020**, *30*, 1908752.

[2] F. Grinnell, *Int. Rev. Cytol.* **1978**, *53*, 65.

[3] D. Hoffman-Kim, J. A. Mitchel, R. V. Bellamkonda, *Annu. Rev. Biomed. Eng.* **2010**, *12*, 203.

[4] B. R. Freedman, A. B. Rodriguez, R. J. Leiphart, J. B. Newton, E. Ban, J. J. Sarver, R. L. Mauck, V. B. Shenoy, L. J. Soslowsky, *Sci. Rep.* **2018**, *8*, 10854.

[5] S. Jana, S. K. L. Levengood, M. Zhang, *Adv. Mater.* **2016**, *28*, 10588.

[6] X. Liao, M. Dulle, J. M. De Souza E Silva, R. B. Wehrspohn, S. Agarwal, S. Förster, H. Hou, P. Smith, A. Greiner, *Science* **2019**, *366*, 1376.

[7] a) A. Sensini, G. Massafra, C. Gotti, A. Zucchelli, L. Cristofolini, *Front. Bioeng. Biotechnol.* **2021**, *9*, 645544; b) J. Jin, Q. Saiding, X. Wang, M. Qin, Y.i Xiang, R. Cheng, W. Cui, X. Chen, *Adv. Funct. Mater.* **2021**, *31*, 2009879.

[8] a) D. Papkov, Y. Zou, M. N. Andalib, A. Goponenko, S. Z. D. Cheng, Y. A. Dzenis, *ACS Nano* **2013**, *7*, 3324; b) A. Arinstein, M. Burman, O. Gendelman, E. Zussman, *Nat. Nanotechnol.* **2007**, *2*, 59.

[9] R. A. O'Connor, G. B. Mcguinness, *Proc. Inst. Mech. Eng., Part H* **2016**, *230*, 987.

[10] S. Agarwal, J. H. Wendorff, A. Greiner, *Polymer* **2008**, *49*, 5603.

[11] M. Mader, M. Helm, M. Lu, M. H. Stenzel, V. Jérôme, S. Agarwal, R. Freitag, A. Greiner, *Biomacromolecules* **2020**, *21*, 4094.

[12] C. Huang, S. Chen, D. H. Reneker, C. Lai, H. Hou, *Adv. Mater.* **2006**, *18*, 668.

[13] M. M. L. Arras, C. Grasl, H. Bergmeister, H. Schima, *Sci. Technol. Adv. Mater.* **2012**, *13*, 035008.

[14] X. Liao, F.-J. Kahle, B. Liu, H. Bässler, X. Zhang, A. Köhler, A. Greiner, *Mater. Horiz.* **2020**, *7*, 1605.

[15] S. Wu, J. Liu, J. Cai, J. Zhao, B. Duan, S. Chen, *Biofabrication* **2021**, *13*, 045018.

[16] S. A. Weiss, J. H. Johnson, *US Patent 4024020*, **1977**.

[17] T. Groth, B. Seifert, G. Malsch, W. Albrecht, D. Paul, A. Kostadinova, N. Krasteva, G. Altankov, *J. Biomed. Mater. Res.* **2002**, *61*, 290.

[18] a) M. Fakhrieh, M. Darvish, A. Ardeshirylajimi, M. Taheri, M. D. Omrani, *J. Cell. Biochem.* **2019**, *120*, 15814; b) A. Ince Yardimci, O. Baskan, S. Yilmaz, G. Mese, E. Ozcivici, Y. Selamet, *J. Biomater. Appl.* **2019**, *34*, 640; c) E. Tanzli, A. Ehrmann, *Appl. Sci.* **2021**, *11*, 6929; d) S.-P. Liu, C.-H. Lin, S.-J. Lin, R.-H. Fu, Y.-C. Huang, S.-Y. Chen, S.-Z. Lin, C. Y. Hsu, W.-C. Shyu, *J. Biomed. Nanotechnol.* **2016**, *12*, 732.

[19] M. R. Ramezani, Z. Ansari-Asl, E. Hoveizi, A. R. Kiasat, *Mater. Chem. Phys.* **2019**, *229*, 242.

[20] S. Cai, S. Wu, W. Yang, W. Liang, H. Yu, L. Liu, *Nanotechnol. Rev.* **2020**, *9*, 971.

[21] a) S. K. Verma, A. Modi, A. K. Singh, R. Teotia, S. Kadam, J. Bellare, *Colloids Surf., B* **2018**, *164*, 358; b) M. Winnacker, A. J. G. Beringer, T. F. Gronauer, H. H. Güngör, L. Reinschlüssel, B. Rieger, S. A. Sieber, *Macromol. Rapid Commun.* **2019**, *40*, 1900091.

[22] a) F. Fey-Lamprecht, W. Albrecht, T. Groth, T. Weigel, U. Gross, *J. Biomed. Mater. Res., Part A* **2003**, *65A*, 144; b) R. K. Sadasivam, S. Mohiyuddin, G. Packirisamy, *ACS Omega* **2017**, *2*, 6556; c) M. N. Sarwar, A. Ullah, M. K. Haider, N. Hussain, S. Ullah, M. Hashmi, M. Q. Khan, I. S. Kim, *Polymers* **2021**, *13*, 510; d) H.-L. Wu, D. H. Bremner, H.-Y. Li, Q.-Q. Shi, J.-Z. Wu, R. -. Q. Xiao, L.-M. Zhu, *Mater. Sci. Eng., C* **2016**, *62*, 702.

[23] E. Pissiotis, L. S. W. Spangberg, *Int. Endod. J.* **1991**, *24*, 249.

[24] ISO 10993-5, "ISO 10993-5: Biological evaluation of medical devices - Part 5: Tests for in vitro cytotoxicity", Beuth Verlag GmbH, Berlin **2009**.

[25] a) G. K. Arbade, J. Srivastava, V. Tripathi, N. Lenka, T. U. Patro, *J. Biomater. Sci., Polym. Ed.* **2020**, *31*, 1648; b) M. M. M. De Paula, N. J. Bassous, S. Afewerki, S. V. Harb, P. Ghannadian, F. R. Marciano, B. C. Viana, C. R. Tim, T. J. Webster, A. O. Lobo, *PLoS One* **2018**, *13*, e0209386; c) L. N. Wang, C. Z. Xin, W. T. Liu, X. L. Xia, S. Q. He, H. Liu, C. S. Zhu, *Arabian J. Sci. Eng.* **2015**, *40*, 2889.

[26] ISO 10993-12, "ISO 10993-12: Biological evaluation of medical devices - Part 12: Sample preparation and reference materials", Beuth Verlag GmbH, Berlin **2004**.

[27] a) S. Cai, S. Wu, W. Yang, W. Liang, H. Yu, L. Liu, *Nanotechnol. Rev.* **2020**, *9*, 971; b) A. Venturato, G. Macfarlane, J. Geng, M. Bradley, *Macromol. Biosci.* **2016**, *16*, 1864.

[28] S. A. Richardson, T. M. Rawlings, J. Muter, M. Walker, J. J. Brosens, N. R. Cameron, A. M. Eissa, *Macromol. Biosci.* **2019**, *19*, 1800351.

[29] a) G. Duan, S. Jiang, V. Jérôme, J. H. Wendorff, A. Fathi, J. Uhm, V. Altstädt, M. Herling, J. Breu, R. Freitag, S. Agarwal, A. Greiner, *Adv. Funct. Mater.* **2015**, *25*, 2850; b) M. Mader, M. Helm, M. Lu, M. H. Stenzel, V. Jérôme, R. Freitag, S. Agarwal, A. Greiner, *Biomacromolecules* **2020**, *21*, 4094; c) M. Mader, V. Jérôme, R. Freitag, S. Agarwal, A. Greiner, *Biomacromolecules* **2018**, *19*, 1663.

[30] C. Leclech, C. Villard, *Front. Bioeng. Biotechnol.* **2020**, *8*, 1198.

ADVANCED
SCIENCE NEWS

www.advancedsciencenews.com

Macro-
molecular
Bioscience

www.mbs-journal.de

[31] X. Ren, L. F. Tapias, B. J. Jank, D. J. Mathisen, M. Lanuti, H. C. Ott, *Biomaterials* **2015**, *52*, 103.

[32] D. Wehlage, H. Blattner, L. Sabantina, R. Bottjer, T. Grothe, A. Rattenholl, F. Gudermann, D. Lutkemeyer, A. Ehrmann, *Tekstilec* **2019**, *62*, 78.

[33] M. Kruse, M. Greuel, F. Kreimendahl, T. Schneiders, B. Bauer, T. Gries, S. Jockenhoevel, *Biomed. Tech.* **2018**, *63*, 231.

[34] a) N. V. Bhagavan, C.-E. Ha, in *Essentials of Medical Biochemistry* (Eds: N. V. Bhagavan, C.-E. Ha), Academic Press, San Diego **2011**, Ch. 10;

b) E. M. Culav, C. H. Clark, M. J. Merrilees, *Phys. Ther.* **1999**, *79*, 308.

[35] D. G. Menter, R. N. Dubois, *Int. J. Cell Biol.* **2012**, *2012*, 723419.

[36] a) A. Curtis, C. Wilkinson, *Biochem. Soc. Symp.* **1999**, *65*, 15; b) M. M. Stevens, J. H. George, *Science* **2005**, *310*, 1135.

[37] D. R. Bogdanowicz, H. H. Lu, *Ann. N. Y. Acad. Sci.* **2017**, *1410*, 3.

[38] J. Uitto, L. Pulkkinen, *Mol. Biol. Rep.* **1996**, *23*, 35.

[39] I. Assanga, *Int. J. Biotechnol. Mol. Biol. Res.* **2013**, *4*, 60.